Acoustic phonon transport through a T-shaped quantum waveguide

2004 J. Phys.: Condens. Matter 16 5049

(http://iopscience.iop.org/0953-8984/16/28/023)

INSTITUTE OF PHYSICS PUBLISHING JOURNAL OF PHYSICS: CONDENSED MATTER

J. Phys.: Condens. Matter **16** (2004) 5049–5059 PII: S0953-8984(04)79113-4

Acoustic phonon transport through a T-shaped quantum waveguide

Wen-Xia Li[1], **Ke-Qiu Chen**[2], **Wenhui Duan**[1,3], **Jian Wu**[1] and **Bing-Lin Gu**[1]

[1] Department of Physics, Tsinghua University, Beijing 100084, People's Republic of China
[2] Laboratory of Organic Solids, Center for Molecular Sciences, Institute of Chemistry, Chinese Academy of Sciences, 100080 Beijing, People's Republic of China

E-mail: keqiuchen@iccas.ac.cn and dwh@phys.tsinghua.edu.cn

Received 8 April 2004
Published 2 July 2004
Online at stacks.iop.org/JPhysCM/16/5049
doi:10.1088/0953-8984/16/28/023

Abstract

We study the transmission coefficient and thermal conductivity for acoustic phonons crossing a T-shaped quantum waveguide at low enough temperatures by use of the scattering-matrix method. Our results show that relatively small changes in the stub length and width can induce strong variations in the phonon transmission and thermal conductivity. Compared with the electron case in such a structure, acoustic phonon transmission and thermal conductivity exhibit some novel and interesting features. The phonon transmission coefficients and thermal conductivity can be artificially controlled by adjusting the parameters of the proposed microstructure.

1. Introduction

Great technological advances in nanoscale lithography and atom-layer epitaxy enable us to obtain various semiconductor nanostructures within which the wavelength or the coherence length of the electron is comparable to or larger than the structure feature size. During the last two decades, electronic transport properties in nanostructures have attracted much attention, especially since the discovery of the quantized conductance phenomenon [1]. One of the most important problems in mesoscopic physics is the understanding of the size effect on the electron transport in quasi-one-dimensional nanostructures. It has been demonstrated that the electronic and optical properties can be engineered to a high degree of precision in quantum structures by using quantum size effects on electrons. This is called bandgap engineering. Because of their novel physical properties in comparison with bulk materials and the potential applications in new devices, a large amount of experimental [2–4] and theoretical [5–8] research on ballistic

[3] Author to whom any correspondence should be addressed.

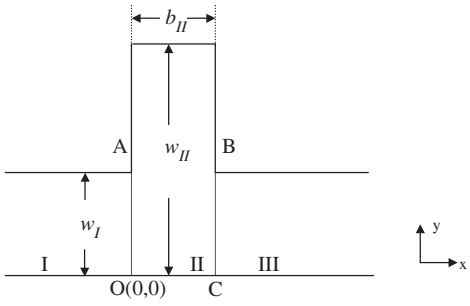

Figure 1. The structure of a T-shaped quantum waveguide.

electron transport in nanostructures with various configurations has been reported over the past few years.

In contrast, little attention has been devoted to the study of phonon thermal conductivity in nanostructures. Thermal conductivity is one of the most important parameters of a semiconductor nanostructure, and it plays a critical role in controlling the performance and stability of nanometre devices. It was not until recently that studies of heat transport associated with phonons in nanostructures have arisen, because for easily fabricated devices the wavelength of a typical thermal phonon becomes comparable to the dimension of the thermal pathway at accessible low temperatures. Several groups [9–11] have derived expressions of thermal conductance for ballistic phonon transport at low enough temperatures in an ideal elastic beam, and found that the thermal conductance at low temperatures is dominated by the lowest modes with zero cutoff frequency and is quantized in a universal unit, $\pi^2 k_B^2 T/3h$, analogous to the well-known $2e^2/h$ electronic conductance quantum. These predictions have been verified experimentally [12]. The effect of surface roughness on the universal thermal conductance in a dielectric quantum wire at low temperatures has also been investigated [13]. The phonon thermal conductance properties in various kinds of nanostructures such as thin films [14], quantum wells [15], superlattices [16–19], nanowires [20–25], one-dimensional glass [26], and nanotubes [27] are now starting to be reported.

Motivated by these works, in this paper we investigate the phonon heat transport in a T-shaped quantum waveguide structure, schematically shown in figure 1. The structure is assumed to be infinite in the longitudinal direction, while the transverse arm (stub) is finite. To our best knowledge, several previous studies on the system mainly focus on the properties of electron transport [28–30]. Many interesting electronic transmission features, such as resonant transmission and resonant reflection, were revealed in the structure. Such a behaviour is due to quantum interference which dominates the ballistic transport regime. These studies also showed that relatively small changes in the stub length can induce strong variations in the electron transmission across the structure. This kind of structure has the potential application to act as a quantum device that may exhibit the proposed quantum transistor effect. It is natural to think whether one can control phonons for the desired thermal properties by adjusting the stub length and other structural parameters, and whether there is an analogy between phonon thermal transmission and electronic transmission in the T-shaped structure. The main purpose of this paper is to answer these questions, which have not been studied theoretically and experimentally up to now. For the structure depicted in figure 1, there exist three types of acoustic modes: the longitudinal polarized **P** mode, the vertically polarized **SV** mode, and the horizontally polarized shear **SH** mode. Their polarization directions are along the x, y, and z directions, respectively. Previously, Wang *et al* [31] theoretically investigated the band structure and the transmission spectrum of an acoustic wave in a periodically stubbed waveguide by using the transfer-matrix method. Numerically, however, they presented the

band structure and transmission spectrum of the out-of-plane (**SH**) mode only under the rigid boundary condition. By using the scattering-matrix method [7, 8, 32] and considering the stress-free boundary condition, in the present paper we calculate the phonon transmission coefficients and thermal conductivity in the T-shaped quantum waveguide, where all of the modes (**SH**, **P**, and **SV** modes) are considered.

This paper is organized as follows. Section 2 gives a brief description of the model and the formulae used in calculations. The calculated results are presented in section 3 with analysis. Finally, a summary is made in section 4.

2. Model and formalism

The structure of a T-shaped quantum waveguide is sketched in figure 1. The main part of the device is a uniform waveguide of the transverse dimension w_{I}, on either side of which is a stub. We label the longitudinal dimension of the stub as b_{II} and its transverse dimension $(w_{\mathrm{II}} - w_{\mathrm{I}})$. Regions I and III are the leads of the device. We assume that the temperatures in regions I and III are T_1 and T_2, respectively; and the temperature difference δT ($\delta T = T_1 - T_2 > 0$) between region I and region III is small. So we can adopt the mean temperature T ($T = (T_1 + T_2)/2$) as the temperature of regions I and III in our calculations. In the practically three-dimensional case, if regions I, II and III have the same thickness, which is small with respect to the other dimensions and also to the wavelength of the elastic waves, there is no mixing of the z mode and a two-dimensional calculation is adequate [9–11, 33].

Considering imperfect coupling at stub-I and stub-III junctions, the thermal conductivity is given by [9, 33]

$$K = \frac{\hbar^2}{k_{\mathrm{B}}T^2}\sum_m \frac{1}{2\pi}\int_{\omega_m}^{\infty} \tau_m(\omega)\frac{\omega^2 \mathrm{e}^{\beta\hbar\omega}}{(\mathrm{e}^{\beta\hbar\omega}-1)^2}\,\mathrm{d}\omega, \tag{1}$$

where $\tau_m(\omega)$ is the energy transmission coefficient from mode m of region I at frequency ω across all the interfaces into the modes of region III. A central issue in predicting the thermal conductivity is then to calculate the transmission coefficient, $\tau_m(\omega)$.

In this paper, we employ the isotropic elastic theory to calculate the transmission coefficient of the acoustic phonon [34]. Under this condition, the phonon modes polarized in the x–y plane are decoupled from the horizontally polarized shear **SH** mode. With the **SH** mode incident into the waveguide, only a single wave-type (**SH**) can exist, as expounded in the elasticity textbook by Graff [34]. When the **P** mode transports into the waveguide, the reflection at the interfaces may lead to the mode conversion, namely its reflection wave and the transmission wave may contain both **P** and **SV** modes. For the **SV** mode incidence, the situation is similar. Then mixing between the **P** mode and the **SV** mode will happen.

First, we consider the simplest case for an **SH** mode incidence at low enough temperatures. The displacement field function satisfies the scalar potential equation

$$\frac{\partial^2\psi}{\partial t^2} - v_{\mathrm{SH}}^2\nabla^2\psi = 0, \tag{2}$$

where the **SH** wave velocity v_{SH} is related to the mass density ρ and elastic stiffness constant C_{44},

$$v_{\mathrm{SH}}^2 = C_{44}/\rho. \tag{3}$$

The stress-free boundary condition at the edges requires that $\hat{n}\cdot\nabla\psi = 0$, with $\hat{n}$ the normal to the edge. For the structure depicted in figure 1, the solution to equation (2) in region ξ (regions I, II, and III) can be expressed as

$$\psi^{\xi}(x, y) = \sum_{n=0}^{N} [A_n^{\xi} e^{ik_n^{\xi}(x-x_{\xi})} + B_n^{\xi} e^{-ik_n^{\xi}(x-x_{\xi})}] \phi_n^{\xi}(y), \tag{4}$$

where x_{ξ} is the reference coordinate along the x direction for region ξ; k_n^{ξ} can be expressed in terms of incident phonon frequency ω, the **SH** wave velocity v_{SH}^{ξ} and the transverse dimension w_{ξ} of region ξ by the energy conservation condition,

$$\omega^2 = k_n^{\xi 2} v_{\mathrm{SH}}^{\xi^2} + \frac{n^2 \pi^2 v_{\mathrm{SH}}^{\xi^2}}{w_{\xi}^2}; \tag{5}$$

$\phi_n^{\xi}(y)$ represents the transverse wavefunction of acoustic mode n in region ξ,

$$\phi_n^{\xi}(y) = \begin{cases} \sqrt{\dfrac{2}{w_{\xi}}} \cos \dfrac{n\pi}{w_{\xi}} y & (n \neq 0) \\ \sqrt{\dfrac{1}{w_{\xi}}} & (n = 0). \end{cases} \tag{6}$$

In principle, the sum over n in equation (4) includes all propagating modes and evanescent modes (imaginary k_n^{ξ}). However, in the real calculations, we take all the propagating modes and a limited number of evanescent modes into account to meet the desired precision. Employing boundary matching (the displacement ψ and the stress $c_{44}\partial\psi/\partial x$ are continuous at the interface of regions I and II ($x = 0$) and the interface of regions II and III ($x = d$)), we obtain the equations for the coefficients in equation (4). Rewriting the resulting equations in the form of a matrix, we can derive the transmission coefficient, τ_m, by the scattering matrix method (for details see [36]).

We now turn to consider the case of **P** wave incidence. Our work focuses on the acoustic phonon thermal transport at low enough temperatures, where only a few of lowest modes can be excited and most of the contribution to the thermal conductivity comes from the zero mode. In this case, the interconversion of **P** and **SV** modes is very small. Thus, we adopt the mixed boundary condition [34] to solve the phonon transport problem. The basic elasticity equations can be resolved by scalar (Φ) and vector (H_z) potential equations [34]. If conditions of plane strain hold in the z direction, we have $u_z = \partial/\partial z = 0$, and

$$u_x = \frac{\partial \Phi}{\partial x} + \frac{\partial H_z}{\partial y}, \tag{7}$$

$$u_y = \frac{\partial \Phi}{\partial y} - \frac{\partial H_z}{\partial x}, \tag{8}$$

where $u_x = u_x(x, y, t)$ and $u_y = u_y(x, y, t)$. Further, we have

$$\nabla^2 \Phi = \frac{1}{v_{\mathrm{L}}^2} \frac{\partial^2 \Phi}{\partial t^2}, \qquad \nabla^2 H_z = \frac{1}{v_{\mathrm{SV}}^2} \frac{\partial^2 H_z}{\partial t^2}, \tag{9}$$

where $v_{\mathrm{L}} = \sqrt{c_{11}/\rho}$ and $v_{\mathrm{SV}} = \sqrt{c_{44}/\rho}$ are the velocities of the **P** wave and the **SV** wave, respectively. The mixed boundary conditions considered here can be expressed by $u_y = T_{xy} = T_{zy} = 0$ at the edges, where T_{xy} and T_{zy} are the stress tensors that can be found in the elasticity textbook [34]. The displacements in different regions ξ (ξ = I, II, or III) can be expressed as

$$u_x^{\xi}(x, y) = \sum_{m=0}^{N} \Bigg\{ (P_{\xi m}^{+} e^{ik_{lm}^{\xi}(x-x_{\xi})} - P_{\xi m}^{-} e^{-ik_{lm}^{\xi}(x-x_{\xi})}) (ik_{lm}^{\mathrm{I}}) \chi_m^{\xi}(y) + (T_{\xi m}^{+} e^{ik_{lm}^{\xi}(x-x_{\xi})} + T_{\xi m}^{-} e^{-ik_{lm}^{\xi}(x-x_{\xi})}) \left(i\frac{n\pi}{w_{\xi}} \right) \chi_m^{\xi}(y) \Bigg\}, \tag{10}$$

and

$$u_y^{\xi}(x,y)=\sum_{m=0}^{N}\Bigg\{(P_{\xi m}^{+}\mathrm{e}^{\mathrm{i}k_{lm}^{\xi}(x-x_{\xi})}+P_{\xi m}^{-}\mathrm{e}^{-\mathrm{i}k_{lm}^{\xi}(x-x_{\xi})})\left(-\frac{m\pi}{w_{\xi}}\right)\eta_m^{\xi}(y)$$
$$+(T_{\xi m}^{+}\mathrm{e}^{\mathrm{i}k_{tm}^{\xi}(x-x_{\xi})}-T_{\xi m}^{-}\mathrm{e}^{-\mathrm{i}k_{tm}^{\xi}(x-x_{\xi})})k_{tm}^{\xi}\eta_m^{\xi}(y)\Bigg\}, \tag{11}$$

where

$$\chi_m^{\xi}(y)=\begin{cases}\sqrt{\dfrac{2}{w_{\xi}}}\cos\left(\dfrac{m\pi}{w_{\xi}}y\right) & (m\neq 0)\\ \sqrt{\dfrac{1}{w_{\xi}}} & (m=0),\end{cases} \tag{12}$$

$$\eta_m^{\xi}(y)=\begin{cases}\sqrt{\dfrac{2}{w_{\xi}}}\sin\left(\dfrac{m\pi}{w_{\xi}}y\right) & (m\neq 0)\\ \sqrt{\dfrac{1}{w_{\xi}}} & (m=0),\end{cases} \tag{13}$$

and

$$\omega^2=(k_{(l,t)m}^{\xi})^2 v_{\mathrm{P,SV}}^{\xi^2}+\frac{m^2\pi^2 v_{\mathrm{P,SV}}^{\xi^2}}{w_{\xi}^2}. \tag{14}$$

Note that the sum over m in equations (10) and (11) includes all propagating modes and a limited number of evanescent modes to meet the desired precision. The boundary conditions at the interfaces ($x=0, b_{\mathrm{II}}$) are now given by

$$u_x^{\mathrm{I(II)}}=u_x^{\mathrm{II(III)}}, \tag{15}$$
$$u_y^{\mathrm{I(II)}}=u_y^{\mathrm{II(III)}}, \tag{16}$$
$$c_{11}\partial u_x^{\mathrm{I(II)}}/\partial x+c_{12}\partial u_y^{\mathrm{I(II)}}/\partial y=c_{11}\partial u_x^{\mathrm{II(III)}}/\partial x+c_{12}\partial u_y^{\mathrm{II(III)}}/\partial y, \tag{17}$$
$$\partial u_x^{\mathrm{I(II)}}/\partial y+\partial u_y^{\mathrm{I(II)}}/\partial x=\partial u_x^{\mathrm{II(III)}}/\partial y+\partial u_y^{\mathrm{II(III)}}/\partial x. \tag{18}$$

Using the scattering matrix method, we can obtain the transmission coefficient. Note that the formulae mentioned above about an incident **P** mode are valid for the case of a **SV** mode incident.

In the calculations, we will employ those values of dielectric constants and density of GaAs referred to [36]: $C_{11}(\mathrm{GaAs})=12.21$ (10^{10} N m^{-2}), $C_{44}(\mathrm{GaAs})=5.99$ (10^{10} N m^{-2}), and $\rho(\mathrm{GaAs})=5317.6$ (kg m^{-3}).

3. Numerical results and discussion

First, we discuss the lowest **SH** acoustic mode incident into the structure depicted in figure 1. It is a character of the acoustic waves that the zero mode with cutoff frequency $\omega=0$ (transversal index $n=0$ in equations (5) and (6)) can propagate through the structure, which is substantially different from the case of electronic transport [28]. This is due to the fact that the acoustic phonon satisfies the stress-free boundary condition, whereas the electron satisfies the rigid boundary condition. For electronic transport, the threshold energy of the lowest mode is positive. That is to say that when the Fermi energy of the electron is lower than the threshold energy, the electron cannot propagate through the structure, and the electron transmission

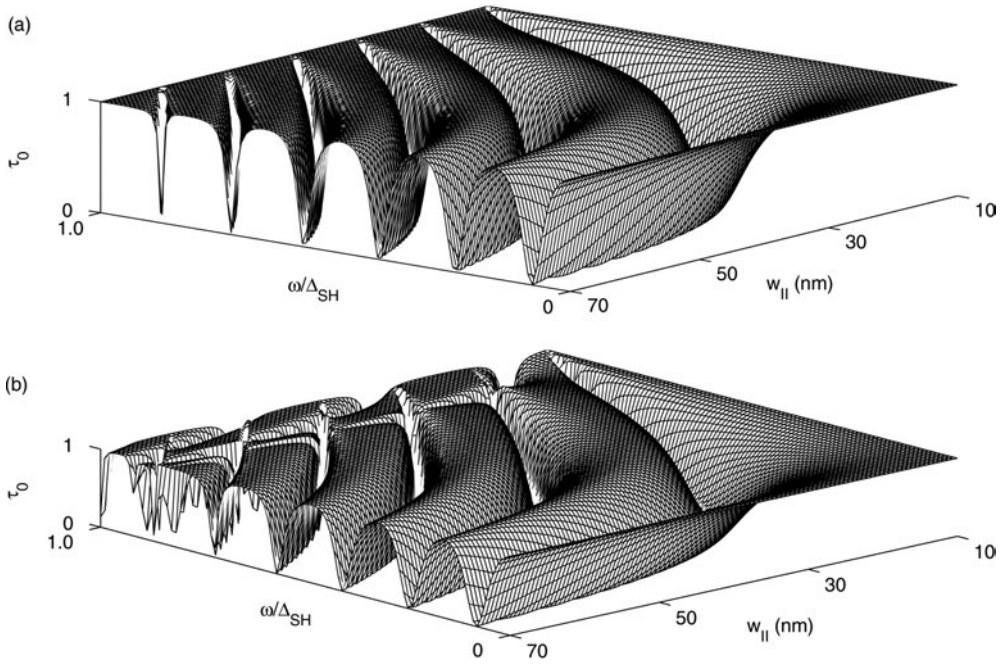

Figure 2. Transmission coefficient versus the length w_{II} and the incident phonon frequency $\omega/\Delta_{\mathrm{SH}}$ for the T-shaped acoustic waveguide structure with $w_{\mathrm{I}} = 10$ nm, where $\Delta = \omega_{n+1} - \omega_n = \pi v_{\mathrm{SH}}/w_{\mathrm{I}}$ (v_{SH} is the acoustic wave velocity in GaAs) represents the splitting of the cutoff frequency between the $(n+1)$th mode and the nth mode in the quantum main waveguide. (a) For $b_{\mathrm{II}} = 10$ nm; (b) for $b_{\mathrm{II}} = 12$ nm.

coefficient is zero. As far as the acoustic phonon is concerned, we find from figure 2 that the transmission coefficients approach unity as $\omega \to 0$, which indicates that the transmission is not influenced by the stub for an incident acoustic phonon with $\omega \to 0$. We also find from figure 2 that for an acoustic phonon with any incident frequency the transmission coefficients approach unity at $w_{\mathrm{II}} = 10$ nm. This is owing to the fact that for the case of $w_{\mathrm{II}} = 10$ nm the stub vanishes and the structure reverts to being a uniform waveguide. From figure 2(a), it can be seen that, for a given frequency, the transmission exhibits a periodic pattern as a function of w_{II}. Figure 2(b) shows the transmission coefficient versus $\omega/\Delta_{\mathrm{SH}}$ and w_{II} for $b_{\mathrm{II}} = 12$ nm $> w_{\mathrm{I}}$. With the increase of the frequency $\omega/\Delta_{\mathrm{SH}}$, the periodic pattern of the transmission coefficient is destroyed. This can be well understood. Increasing the stub width b_{II} leads to a lowering of the cutoff frequency of the propagating wave along the stub. Thus, more than one transverse mode can exist in the stub. These modes will couple with the incident modes. In general, the more that modes couple with the incident modes in the stub, then the more complex the transmission spectra. This is the reason why figure 2(b) displays a distorted transmission pattern.

To see more clearly the dependence of the transmission coefficients on the stub length, we show the transmission coefficient as a function of w_{II} for different frequencies in figure 3. We find that a relatively small change in w_{II} can induce dramatic changes in the transmission for a wide range of frequencies and appropriate choice of dimensions. When only the lowest mode with transversal index $n = 0$ exists in the stub, the transmission spectra present periodic behaviour and the period is one half of the wavelength. It is interesting to note that similar phenomena are observed in electronic transmission [28]. It is known that the propagation

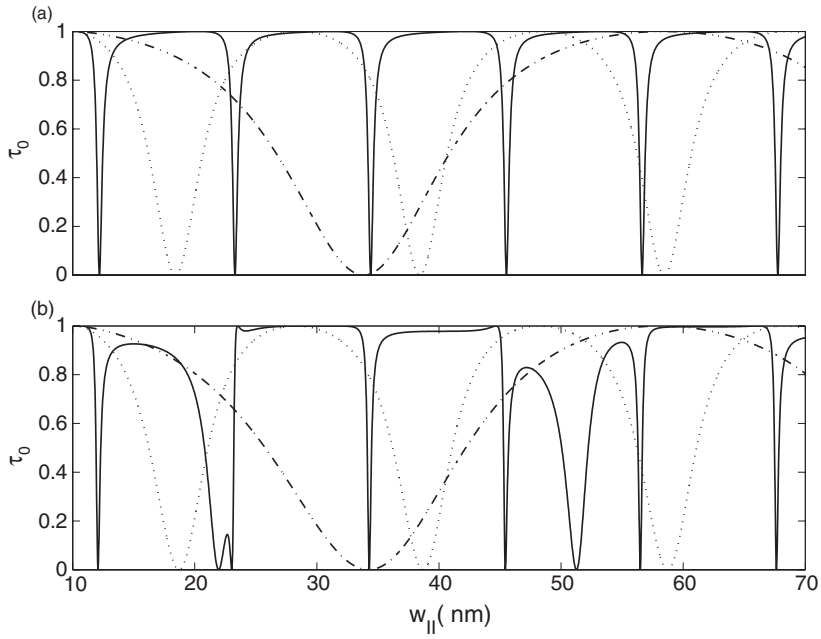

Figure 3. The transmission coefficient as a function of the stub length $w_{\rm II}$, for different frequencies in figure 2: the dot–dashed, dotted, and solid curves in (a) and (b) correspond to $\omega/\Delta_{\rm SH} = 0.2$, 0.5, and 0.9 in figures 2(a), (b), respectively.

wave and reflected wave with same wavenumber, $k = \sqrt{\omega^2/v^2 - n^2\pi^2/b_{\rm II}^2}$, in the stub will couple together and form a standing wave inside the stub. The wave reflected from the stub will couple with the wave in the main waveguide. When the phase shift between the incident wave in the main waveguide and the reflected wave from the stub is just equal to $2n\pi$, the transmission in the main waveguide will be reinforced and $\tau = 1$; while the phase shift is $(2n+1)\pi$, the transmission coefficient, τ, is zero. Consequently, a periodic oscillation appears in the transmission spectra and the period, $\Delta w_{\rm II}$, of the oscillation can be obtained from $2k\Delta w_{\rm II} = 2\pi$, namely $\Delta w_{\rm II} = \pi/k = \lambda/2$. This is confirmed by figure 3. These results could be very useful for the design of phonon devices.

Now we investigate the transmission character of **P** wave incidence. Figure 4 shows some new transmission characters, different from those in figure 2, due to the mode conversion and mode mixing effect. Zero transmission only occurs at $0 < \omega/\Delta_{\rm P} < 0.7$ and at the frequency range only the zero modes exist in the waveguide. At frequency $\omega = 0.7\Delta_{\rm P}$, where the first **SV** mode starts to be excited, there is a rapid decrease in transmission coefficient. From figure 4, we find that when $b_{\rm II} \leqq 7$ nm the transmission spectra still exhibit a quasi-periodic pattern as a function of $w_{\rm II}$ through the explored frequency scope. However, there are more resonance transmission peaks in figure 4(a) than in 2(a), which indicates that the mode mixing effect can reduce the resonance period. When $b_{\rm II} > 7$ nm, the periodicity is destroyed for the higher frequency (see figure 4(b)). We also find that when only zero modes are available in the stub, the transmission spectra of **P** wave will change periodically with the length of the stub; while more than one kind of mode exists in the stub, the periodicity will be destroyed, similar to the case of the **SH** wave. It is known that the vibration frequency of the acoustic phonon is very small at very low temperatures, and only a small amount of mode conversion can occur

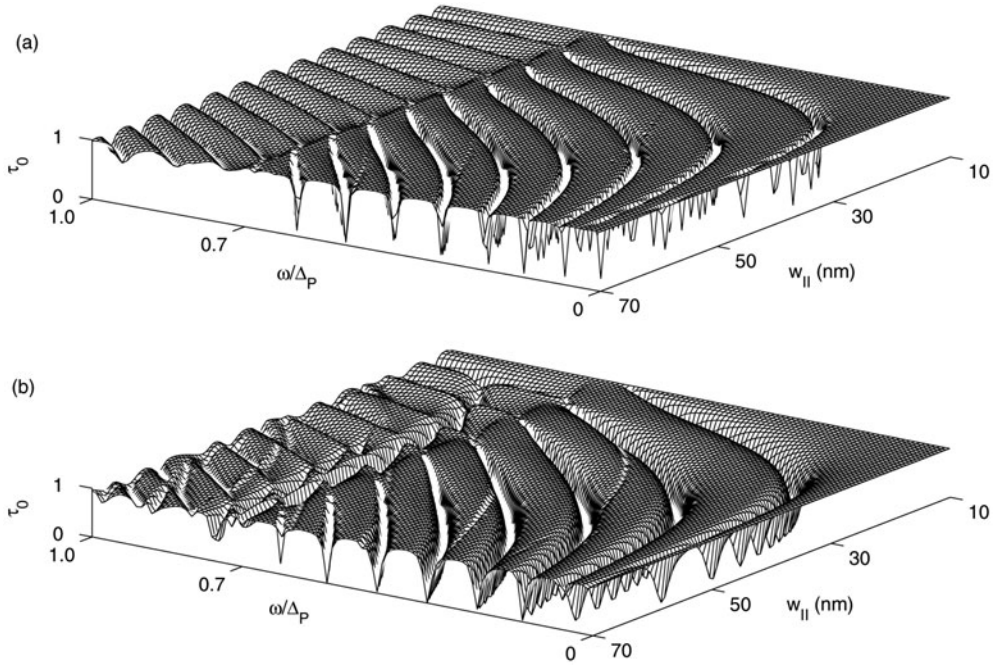

Figure 4. Transmission coefficient versus the length w_{II} and the incident phonon frequency $\omega/\Delta_{\mathrm{P}}$ for the T-shaped acoustic waveguide structure with $w_{\mathrm{I}} = 10$ nm, where $\Delta = \omega_{n+1} - \omega_n = \pi v_{\mathrm{P}}/w_{\mathrm{I}}$ (v_{P} is the acoustic wave velocity in GaAs) represents the splitting of the cutoff frequency between the $(n+1)$th mode and the nth mode in the quantum main waveguide. (a) For $b_{\mathrm{II}} = 7$ nm; (b) for $b_{\mathrm{II}} = 10$ nm.

at each interface. So the quasi-period transmission is not essentially destroyed by the mode mixing effect. This also indicates that it is reasonable for us to solve the phonon transmission by adopting a mode mixed boundary condition.

Now we turn to investigate the acoustic phonon thermal conductivity in the T-shaped waveguide structure. At very low temperatures, zero mode thermal transport is dominant. The mode mixing effect on thermal conductivity is small. Our calculations also show that at a low temperature the thermal conductivity of the **SH** wave has similar features to those of the **P** wave. We give the thermal conductivity of **p** wave incidence considering mode mixing as follows.

Figure 5 shows the thermal conductivity divided by temperature reduced by the zero-temperature universal $\pi^2 k_{\mathrm{B}}^2/3h$ as a function of the reduced temperature $k_{\mathrm{B}}T/\hbar\Delta_{\mathrm{P}}$. As seen from figure 5, for the given temperature range, the reduced thermal conductivity K/T is dominated by the first few acoustic modes, especially the zero acoustic mode. When T approaches zero, only the zero mode can be excited and thus only the zero mode contributes to the thermal conductivity. Comparing curves (b) and (c) with (d), the reduced thermal conductivity of mode 1 or 2 increases with increasing temperature, while that of the zero mode seems to be insensitive to the temperature except at the very low temperatures regime where it rapidly decreases with increasing temperature. The dramatic change of the thermal conductivity of the zero mode at very low temperatures is considered to be the result of the resonance coupling of the zero mode in the main wire and the zero mode of the stub, which leads to the lower transmission coefficient for the given parameters. Correspondingly, a decrease

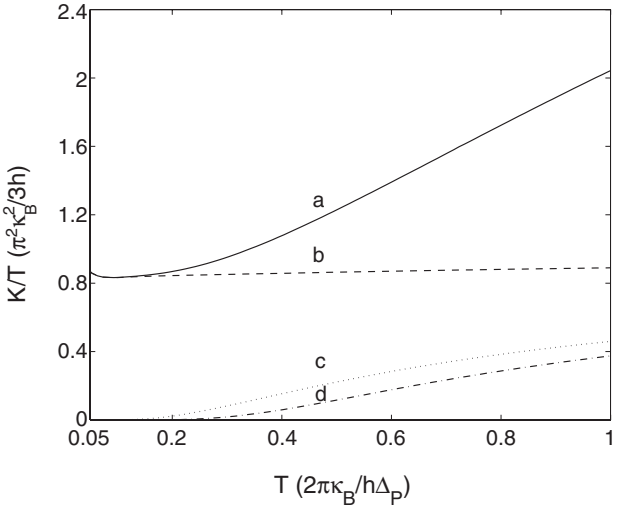

Figure 5. Thermal conductivity divided by temperature, K/T, which is reduced by the zero-temperature universal value $\pi^2 k_B^2/3h$, as a function of the reduced temperature $k_B T/\hbar\Delta_P$. Here, we take $w_I = b_{II} = 10$ nm, and $w_{II} = 20$ nm. Curve (a) corresponds to the total conductivity, and curves (b)–(d) correspond to the conductivity of mode 0, 1, and 2, respectively.

in the reduced total thermal conductivity appears. Moreover, it is worth pointing out that the reduced total thermal conductivity increases linearly with temperature.

In figure 6, we envisage the effect of the stub width on the reduced total thermal conductivity K/T. Figure 6 shows that with the increase of the stub width b_{II}, the reduced thermal conductivity shifts down. This can be understood easily. The larger the value of b_{II}, the more transverse modes are available in the stub, and the stronger the scattering to the transmission. Consequently, the transmission coefficient and thermal conductivity decrease. Therefore, we can control the transmission characteristics by adjusting the transversal modes in the stub, namely by changing the stub width b_{II}. This appears to be important for applications in devices. In figure 7, we explore the influence of w_{II} on the reduced total thermal conductivity K/T. It is clearly seen from curve (a) that no reduction in the thermal transport occurs, and a plateau at the universal value $\pi^2 k_B^2/3h$ appears at low temperature regime. This is due to the fact that the T-shaped structure reverts to a uniform waveguide structure, in which no scattering happens for ballistic transport in such a uniform waveguide. The forming of the plateau further shows that the reduced thermal conductivity of zero mode is insensitive to the temperature. With the increase of the stub length, the reduced total thermal conductivity decreases noticeably, which indicates that we may adjust the thermal conductivity by changing the stub length.

4. Summary

In this paper, we have presented a numerical calculation of the phonon transmission and thermal conductivity in a T-shaped waveguide structure. We observe some novel and interesting characteristics for acoustic phonon transmission and thermal conductivity in the structure, substantially different from the case of electronic transport. The stress-free boundary condition of an acoustic phonon leads to the propagation of the zero mode, and when only the zero mode is available in the stub, the transmission spectra will change periodically with the length of the stub. However, while more than one mode exists in the stub, the periodicity will be destroyed. The thermal conductivity is not zero when $T \to 0$. Moreover, the reduced thermal conductivity of the excited acoustic modes increases with temperature significantly, while that of the zero mode seems to be insensitive to temperature except at the very low temperature

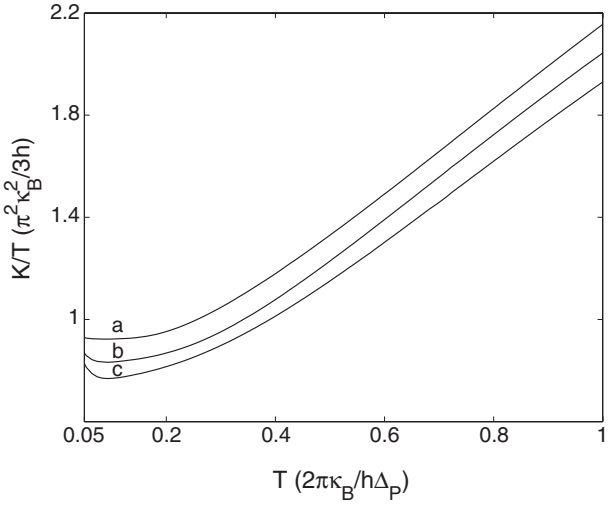

Figure 6. The thermal conductivity divided by temperature reduced by the zero-temperature universal $\pi^2 k_B^2/3h$ as a function of the reduced temperature $k_B T/\hbar\Delta_P$ for different b_{II}. Curves (a), (b), and (c) correspond to $b_{II} = 5$, 10, and 15 nm, respectively. Here, we take $w_I = 10$ nm, and $w_{II} = 20$ nm.

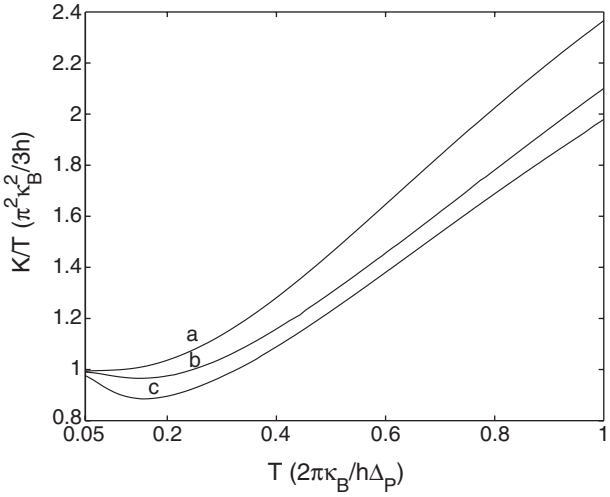

Figure 7. The thermal conductivity divided by temperature reduced by the zero-temperature universal $\pi^2 k_B^2/3h$ as a function of the reduced temperature $k_B T/\hbar\Delta_P$ for different w_{II}. Curves (a), (b), and (c) correspond to $w_{II} = 10$, 12, and 14 nm, respectively. Here, we take $w_I = 10$ nm, and $b_{II} = 10$ nm.

regime where it rapidly decreases with the increase of temperature. These results show that the transmission probabilities and thermal conductivity for acoustic phonons are sensitive to the structural parameters. It is suggested that adjusting the structural parameters is an effective way to control the transmission properties and the thermal conductivities of structures to match practical requirements in devices.

Acknowledgments

This work was supported by the National Natural Science Foundation of China (Grant Nos. 10104010 and 10325415), the National High Technology Research and Development Program of China (Grant No 2002AA311153), the Ministry of Education of China, and by the Chinese Academy of Sciences.

References

[1] Van Wee B J, van Houten H, Beenakker C W J, Williamson J G, Kouwenhoven L P, van der Marel D and Foxon C T 1998 *Phys. Rev. Lett.* **60** 848
[2] Wu J C, Wybourne M N, Yindeepol W, Weisshaar A and Goodnick S M 1991 *Appl. Phys. Lett.* **59** 102
[3] Hieke K and Ulfward M 2000 *Phys. Rev.* B **62** 16727
[4] Worschech L, Xu H Q, Forchel A and Samuelson L 2001 *Appl. Phys. Lett.* **79** 3287
[5] Szafer A and Stone A 1989 *Phys. Rev. Lett.* **62** 300
[6] Leng M and Lent C S 1993 *Phys. Rev. Lett.* **71** 137
[7] Sheng W D 1997 *J. Phys.: Condens. Matter* **9** 8369
[8] Xu H Q 1995 *Phys. Rev.* B **52** 5803
Xu H Q 2002 *Appl. Phys. Lett.* **80** 853
[9] Rego L G C and Kirczenow G 1998 *Phys. Rev. Lett.* **81** 232
[10] Angelescu D E, Cross M C and Roukes M L 1998 *Superlatt. Microstruct.* **23** 673
[11] Blencowe M P 1999 *Phys. Rev.* B **59** 4992
[12] Schwab K, Henriksen E A, Worlock J M and Roukes M L 2000 *Nature* **404** 974
[13] Santamore D H and Cross M C 2001 *Phys. Rev. Lett.* **87** 115502
Santamore D H and Cross M C 2001 *Phys. Rev.* B **63** 184306
[14] Philip J, Hess P, Feygelson T, Butler J E, Chattopadhyay S, Chen K H and Chen L C 2003 *J. Appl. Phys.* **93** 2164
[15] Balandin A and Wang K L 1998 *Phys. Rev.* B **58** 1544
[16] Lee S M, Cahill D G and Venkatasubramanian R 1997 *Appl. Phys. Lett.* **70** 2957
[17] Chen G 1998 *Phys. Rev.* B **57** 14958
[18] Bies W E, Radtke R J and Ehrenreich H 2000 *J. Appl. Phys.* **88** 1498
[19] Simkin M V and Mahan G D 2000 *Phys. Rev. Lett.* **84** 927
[20] Glavin B A 2001 *Phys. Rev. Lett.* **86** 4318
[21] Balandin A 2000 *Phys. Low-Dimens. Struct.* **1/2** 1
[22] Volz S, Lemonnier D and Saulnier J B 2001 *Microstruct. Thermophys. Eng.* **5** 191
[23] Zou J and Balandin A 2001 *J. Appl. Phys.* **89** 2932
[24] Chen G 2000 *Int. J. Thermal Sci.* **39** 471
[25] Chen G and Zeng T 2001 *Microstruct. Thermophys. Eng.* **5** 71
[26] Leitner D M 2001 *Phys. Rev.* B **64** 094201
[27] Kim P, Shi L, Majumdar A and McEuen P L 2001 *Phys. Rev. Lett.* **87** 215502
[28] Soles F, Macuucci M, Ravaioli U and Hess K 1989 *Appl. Phys. Lett.* **54** 350
Soles F, Macuucci M, Ravaioli U and Hess K 1989 *J. Appl. Phys.* **66** 3892
[29] Weisshaar A, Lary J, Goodnick S M and Tripathi V K 1989 *Appl. Phys. Lett.* **55** 2114
[30] Wu H, Sprung D W L, Martorell J and Klarsfeld S 1991 *Phys. Rev.* B **44** 6351
[31] Wang X F, Kushwaha M S and Vasilopoulos P 2001 *Phys. Rev.* B **65** 035107
[32] Tamura H and Ando T 1991 *Phys. Rev.* B **44** 1792
[33] Cross M C and Lifshitz R 2001 *Phys. Rev.* B **64** 085324
[34] Graff K 1991 *Wave Motion in Elastic Solids* (New York: Dover)
[35] Li W X, Chen K Q, Duan W H, Wu J and Gu B L 2003 *J. Phys. D: Appl. Phys.* **36** 3027
[36] Chen K-Q, Wang X-H and Gu B-Y 2000 *Phys. Rev.* B **61** 12075